Sampling Headwater Stream Networks for Spatial Autocorrelation Detection and Autocovariance Parameter Estimation

Journal:	*Environmetrics*
Manuscript ID:	env-10-0145
Wiley - Manuscript type:	Research Article
Date Submitted by the Author:	15-Dec-2010
Complete List of Authors:	Som, Nicholas; Oregon State University, Forest Ecosystems and Society Ganio, Lisa; Oregon State University, Forest Ecosystems and Society Gresswell, Robert; U.S. Geological Survey, Northern Rocky Mountain Science Center Hockman-Wert, David; U.S. Geological Survey, Forest & Rangeland Ecosystem Science Center
Keywords:	Spatial Autocorrelation, Stream Networks, Sampling, Tributary

Sampling Headwater Stream Networks for Spatial Autocorrelation Detection and Autocovariance Parameter Estimation

Nicholas A. Som Lisa M. Ganio Robert E. Gresswell
David Hockman-Wert

December 15, 2010

N. A. Som is a Post-Doctoral Research Associate, Department of Forest Ecosystems and Society, College of Forestry, Oregon State University, Corvallis, OR, 97331 (e-mail nicholas.som@oregonstate.edu). L. M. Ganio is an Associate Professor, Department of Forest Ecosystems and Society, College of Forestry, Oregon State University, Corvallis, OR, 97331. R. E. Gresswell is a Research Biologist, U.S. Geological Survey, Northern Rocky Mountain Science Center, Bozeman, MT, 59715. D. Hockman-Wert is a Biologist, U.S. Geological Survey, Forest and Rangeland Ecosystem Science Center, Corvallis, OR, 97331.

1 Abstract

Spatial autocorrelation is common in data collected for ecological studies, and the use of statistical models for spatial autocorrelation has evolved. Initially, these models were used to improve linear model parameter estimation uncertainty, but more recently ecologists have considered spatial autocorrelation as a valuable tool for describing ecological patterns. The structure and water-driven continuity of stream-networks makes these landscapes unique, and has prompted development of new models for describing spatial autocorrelation within these networks. We evaluate the spatial autocorrelation detection and parameter estimation of four sampling protocols applied to complete censuses of coastal cutthroat trout (*Oncorhynchus clarkii clarkii*) habitat unit fish counts. We consider two cluster- and two non cluster-based sampling protocols. Spatially distributed clusters were the most apt to contain spatial autocorrelation. Spatial autocorrelation detection was also associated with headwater basin attributes. Differences among sampling protocols in regards to autocorrelation parameter estimation were less distinct.

2 Introduction

Attention to patterns of spatial autocorrelation in ecology has shifted dramatically. Geostatistical methods were first used to account for spatial autocorrelation in order to estimate the mean, assess relationships between explanatory and response variables, or make predictions at unobserved locations. More recently, ecologists have focused attention on the spatial process itself, recognizing the implications of variance patterns across their systems of study as valuable explanatory and predictive tools, rather than simply sources of background variation (Pickett and Cadenasso, 1995). The realization that spatial patterns are important components of ecosystems has rendered the study of spatial heterogeneity important in its own right (Legendre, 1993).

Realizations of this shift include Ettema and Wardle (2002) recognizing spatial variability as a key, rather than nuisance, to understanding the structure and function of soil biodiversity. Other studies relating spatial variability to soil variables include Russo and Bresler (1981), Schlesinger et al. (1996), Solie et al. (1999), Grundmann and Debouzie (2000), Muneto et al. (2001), and Blair (2005). Examples from forest plants include Mast and Veblen (1999) and Bouza et al. (2002). Rossi (2003) used spatial autocorrelation to study earthworms. There has also been much work utilizing spatial heterogeneity in aquatic ecosystems that include river or stream nutrients and water quality (Cressie and Majure, 1997; Little et al., 1997; Rathbun, 1998; Peterson and Urquhart, 2006; Dent and Grimm, 1999; Cressie et al., 2006), tropical sea plankton (Bulit et al., 2003, 2004), seabirds (Huettmann and Diamond, 2006), aquatic invertebrates (Downes et al., 1993; Lloyd et al., 2005), stream substrate composition (Rice and Church, 1998; Venditti and Church, 2005), stream temperature (Gardner et al., 2003), and riverine fish (Torgersen and Close, 2004; Isaak and Thurow, 2006; Ganio et al., 2005; Neville et al., 2006).

The autocovariance function can be used to model the decaying autocovariance (C(h)) between observations as distance between them (h) increases. The geostatistical model for C(h) often contains the range, nugget, and partial sill parameters (Schabenberger and Gotway, 2005). The range and partial sill parameters describe the rate of covariance decay with h, and the partial sill and nugget parameters describe the covariance when h is zero. The autocorrelation function (R(h)) standardizes the autocovariance function between 0 and 1, and can also be used to describe this relationship. $R(h) = C(h)/C(0)$, and utilizes the three autocovariance parameters simultaneously.

Spatially explicit data are needed to describe and compare the spatial autocovariance patterns of ecological phenomenon. Data are obtained through sampling, and sampling is the focus of this work. Although spatial statistical methods are traditionally used to analyze data that have already been collected, they can also be used to design sampling programs (Cooper et al., 1997). Regardless of the analysis goal, estimation of spatial autocorrelation is among the essential steps in any geostatistical analysis (Gascuel-Odoux and Boivin, 1994). Because inferences for spatial data are affected substantially by the configuration of the network of sites where measurements are taken (Zimmerman, 2006), a suboptimal selection of sampling locations can result in greater covariance function uncertainty (Russo and Jury, 1987). Furthermore, efficient spatial autocorrelation parameter estimation is significantly affected by the sampling design (Muller and Zimmerman, 1999), and therefore, it is imperative that efficient sampling designs be investigated.

There is a solid and consistent body of work on estimating spatial autocorrelation parameters for geostatistical data. Zimmerman (2006) found that for efficient estimation of covariance parameters a design should have a large number of short and long distances between sample points (lags). This design can be achieved via regularly spaced clusters, many of which lie along the periphery of the sampling space. Similarly, Zhu and Zhang (2006) conclude that designs including closely spaced points lead to more efficient estimation of covariance parameters, and work from Zhu and Stein (2005) found designs with clusters of sampling locations more efficient than non-clustered completely regular or simple random sampling designs. The most efficient designs for spatial autocorrelation parameter estimation evaluated by Muller and Zimmerman (1999) also included many tightly clumped groups of sampling locations. Assessing maximum likelihood (ML) and restricted maximum likelihood (REML) for estimating autocovariance parameters, Irvine et al. (2007) also found a cluster-based design provided the smallest inter-quartile range for estimates of the autocorrelation function, compared to regular lattice or random designs for estimating autocovariance parameters.

The above results are satisfactory for covariance parameter estimation in landscape studies. They may not, however, be sufficient for stream ecology studies. Each stream network consists of linear segments within a unique branching structure. Water flow connects segments, but connectivity between segments varies because of inputs from upstream segments at each tributary junction. This notion is most succinctly concluded by Hynes (1975): every stream is likely to be an individual. These traits have led to further developments in the study of autocovariance methods for stream networks. Ver Hoef et al. (2006) used moving average constructions to develop spatial autocovariance models for stream networks based on stream distance that also incorporate relative flow contribution between stream segments. Additionally, new methods for sampling spatially distributed resources, such as generalized random-tessellation stratified (GRTS) designs, that lead to spatially well distributed probability samples (Stevens Jr. and Olsen, 2004) have been created. These developments allow investigation of covariance parameter estimation performance for stream networks in light of new sampling and analysis methods for stream network spatial data.

Tributary confluences are a common element among stream networks, and there is growing evidence that confluences affect spatial processes in streams. Poole (2002) suggests the physical context of a stream segment is an important consideration for understanding primary drivers of biotic community composition at stream locations. Confluences are areas of increased morphological (Benda et al., 2004b), chemical, and biological stream heterogeneity (Kiffney et al., 2006). Benda et al. (2004a) conclude that the probability of a tributary impact on mainstem morphology increases with the tributary size relative to the mainstem. They link this relationship to the spatial distribution of fluvial geomorphic processes and forms. Physical attributes relating to tributary inputs affect fish habitat (Ferguson et al., 2006; Torgersen et al., 2008), and biological responses to increased levels of environmental variability near confluences are expected (Rice et al., 2006).

Given the benefit of clustered sampling for covariance parameter estimation, and the role that confluences play in the spatial heterogeneity of stream networks, we hypothesize that sampling designs assigning clusters of sampling locations centered at tributary junctions might improve covariance parameter estimation. The previously cited studies evaluating performances of sampling designs for autocovariance parameter estimation used simulated data, but to our knowledge sampling design performance has not been investigated using real-world data. Pooler and Smith (2005) censused a 40 x 33 m section of the Cacapon River in West Virginia to evaluate sampling designs for estimating the distribution and abundance of freshwater mussels. In a similar manner, we will compare the spatial autocovariance parameter estimates obtained by re-sampling census data. Samples from tributary focused clusters, spatially distributed clusters, and two non-clustered sampling protocols will be compared in a design-based analysis of autocovariance detection and parameter estimation.

3 Methods

3.1 40 Basins Dataset

Coastal cutthroat trout (*Oncorhynchus clarkii clarkii*) were continuously sampled in 40 watersheds located west of the Cascade Mountains in Oregon (Gresswell et al., 2004). The basins are located above barriers to anadromous fish migration and are part of a larger study examining the effects of landscape pattern on isolated coastal cutthroat trout populations. Each of the 40 basins was randomly selected from a population of 269 second- and third-order catchments and surveyed through the entire fish-bearing extent (Gresswell et al., 2006). Adult coastal cutthroat trout abundance was assessed with single-pass electrofishing without blocknets (Bateman et al., 2005) in all pools and cascade habitat units in each watershed. These data constitute a census of the habitat units within each headwater basin. Twelve headwater basins whose fish-bearing extent encompassed between three and ten tributary junctions were selected for this analysis. We note that these data represent a one time snap-shot of habitat unit fish-counts, and that habitat unit fish counts can change quickly and dramatically over time (Bateman et al., 2005).

3.2 Autocovariance Models for the Census Data

We begin by establishing census data autocovariance parameters for each of i basins. These parameter values are used to construct census values of $R_i(h)$. Values of $\hat{R}_i(h)$ from each of the sampling protocols described in the next section are compared to these $R_i(h)$ values.

We consider four candidate autocovariance models for the census data from each basin. All habitat unit fish counts were transformed via a $logarithm_e(datum + 1)$ transformation. The four autocovariance models for isotropic and stationary spatial processes come from two different classes. The first class represents geostatistical models that use pairwise Euclidean distances among habitat units. We first consider the exponential with nugget autocovariance model

$$C(h) = \begin{cases} \theta_0 + \theta_1 & \text{if } h = 0 \\ \theta_1 exp(-3h\theta_2^{-1}) & \text{if } h > 0 \end{cases} \tag{1}$$

where h is the Euclidean distance between observations, θ_0 is the nugget parameter, θ_1 is the partial sill parameter, and θ_2 is the practical range parameter. The practical range is defined as the distance at which correlation between observations $\approx 5\%$ (Schabenberger and Gotway, 2005).

We also considered the spherical with nugget autocovariance model

$$C(h) = \begin{cases} \theta_0 + \theta_1 & \text{if } h = 0 \\ \theta_1 \left[1 + .5(h\theta_2^{-1})^3 - 1.5h\theta_2^{-1}\right] & \text{if } 0 < h < \theta_2 \\ 0 & \text{if } \theta_2 \leq h \end{cases} \tag{2}$$

where h is the Euclidean distance between observations, θ_0 is the nugget parameter, θ_1 is the partial sill parameter, and θ_2 is the range parameter.

The second class of spatial autocovariance models are tail-up spatial moving average models for stream networks (Ver Hoef et al., 2006) which use in-stream distances. For moving average in-stream models, the exponential model describing the covariance between an observation s_i downstream of observation s_j is

$$C(s_i, s_j) = \begin{cases} \theta_0 + \theta_1 & \text{if } h = 0 \\ \theta_1 exp(-3h\theta_2^{-1})\sqrt{w_{i,j}} & \text{if } h > 0 \text{ and } s_i,\ s_j \text{ are flow connected} \\ 0 & \text{if } s_i,\ s_j \text{ not flow connected} \end{cases} \tag{3}$$

where h is the distance along the stream network between locations s_i and s_j, $w_{i,j}$ is the proportion of water flow the stream segment containing s_i receives from the segment containing s_j, and with θ_0, θ_1, and θ_2 as in (1). The moving average analog to (2) is

$$C(s_i, s_j) = \begin{cases} \theta_0 + \theta_1 & \text{if } h = 0 \\ \theta_1 \left[1 + .5(h\theta_2^{-1})^3 - 1.5h\theta_2^{-1}\right]\sqrt{w_{i,j}} & \text{if } 0 < h < \theta_2 \text{ and } s_i,\ s_j \text{ are flow connected} \\ 0 & \text{if } \theta_2 \leq h \text{ or } s_i,\ s_j \text{ not flow connected} \end{cases} \tag{4}$$

with h and $w_{i,j}$ as in (3) and θ_0, θ_1, and θ_2 as in (2). These models differ from the geostatistical models in the distance measure used, and in two other ways. First, the autocovariance between locations is weighted proportionally to the amount of stream flow the downstream location receives from the upstream location. Second, two habitat units are only considered autocorrelated if they are connected via water flow through the stream network. See Ver Hoef et al. (2006) and Peterson et al. (2007) for more details. Relative flow contribution was not directly measured for each location in the watershed. The proportion of the upstream watershed area drained by each stream segment was used to weight the moving average autocovariance functions at each tributary confluence (Peterson et al., 2007). We computed all confluence weights and in-stream distances via the FLoWS ArcGIS toolbox (http://www.nrel.colostate.edu/projects/starmap/flows_index.htm).

Maximum likelihood equations were optimized to obtain parameter values, given the census data, for each basin using R code from Ver Hoef and Peterson (2007). Akaike's information criterion (AIC) values were used to determine which candidate model was best supported by the data (Zuur et al., 2009). If necessary, we also considered the relative structured variability (RSV) (Schabenberger and Gotway, 2005) of each candidate model, where $RSV = \frac{\theta_0}{\theta_0+\theta_1}$. The autocovariance model with the highest RSV was chosen if any AIC values from the four autocovariance models were within 2 AIC units of the best fitting model.

For reference, we also fit a model that assumed each observation within each basin was independent and not spatially autocorrelated. AIC values from these models and empirical semivariograms were used to ascertain the presence of autocorrelation in the census data for each basin.

We used the selected spatial autocovariance model from each of the i basins to calculate $R_i(h)$ at distances (h) of 25, 100, and 200 m. We chose these lag values to represent relatively short, medium, and long distances between sampling locations within the basins.

3.3 Sampling Protocols

We now describe the four sampling protocols and resampling process used to compare the spatial autocorrelation detection and parameter estimation performance of each protocol. Evidence of spatial autocorrelation and $\hat{R}_i(h)$ values computed from the autocovariance parameter estimates of each sample will be assessed.

Two cluster-based, and two non cluster-based, sampling protocols were employed in this study (Figure 1). For notation, m is the number of clusters, l is the number of habitat units within each sample cluster, and $n = l * m$ is the sample size.

The first sampling protocol is simple random sampling (SRS) without replacement. We chose n habitat units randomly from the habitat units for each basin using the *sample* function in R statistical computing software (R Development Core Team, 2005).

The second sampling protocol is the generalized random tessellation stratified (GRTS) methodology aimed to create spatially balanced probability samples (Stevens Jr. and Olsen, 2004). We chose n habitat units from the habitat units for each basin using the *spsurvey* R package (Kincaid et al., 2008) for the implementation of GRTS sampling.

The third sampling protocol, referred to as Mod.GRTS, is a modified GRTS procedure that we applied to select spatially balanced clusters of sampled habitat units throughout the headwater basins. We used *spsurvey* to select a spatially distributed set of m cluster centroids. At each centroid, a continuous cluster sample of size l was obtained by selecting $\frac{l}{2}$ habitat units upstream and including the centroid, and $\frac{l}{2}$ habitats units directly downstream of the centroid. Should $\frac{l}{2}$ habitat units in either direction result in the encountering of a tributary junction, the remaining units yet unassigned were split among the two other segments leading from the junction. The total number of centroids chosen corresponded to the number of tributary junctions within each headwater basin for comparison with the TOCCSIC sampling protocol described below.

The fourth sampling protocol is tributary junction only, continuous cluster sampling in catchments (TOCCSIC). Moving away from m tributary junctions along each stream segment $\frac{l}{3}$ consecutive habitat units were selected for sampling. Should $\frac{l}{3}$ be sufficiently large in a direction as to encounter another tributary junction, the remaining units were split among the habitat units of the other two adjoining stream segments.

3.4 Resampling

As habitat unit surveys in each headwater basin represent a complete census, a sample of habitat units from each basin was drawn according to each of the four sampling protocols. For each combination of basin and sampling protocol, a sample of size n was drawn D times where

$$D = max(50, tCm); \text{ where } tCm = \frac{t!}{m!(t-m)!} \quad (5)$$

for the GRTS, Mod.GRTS, and SRS protocols, and t is the total number of tributary junctions within each headwater basin. There were only tCm unique samples possible for the TOCCSIC design, and all $D = tCm$ possible samples were generated. To investigate performances of the Mod.GRTS and TOCCSIC sampling protocols under different cluster sizes, we used sample sizes of 48 habitat units (2 clusters of 24 units or 4 clusters of 12 units), 72 habitat units (2 of 36, 3 of 24, 4 of 18, and 6 of 12), and 144 habitat units (4 of 36 and 6 of 24) (Table 1).

Two autocovariance models were fit to each sample. The first is the autocovariance model chosen for the habitat unit census in that basin, and is hereafter referred to as a spatial autocovariance (SAC) model. The second model, hereafter referred to as simple linear regression (SLR), assumes no spatial autocorrelation in the sample and includes a single variance parameter. We estimated model parameters using maximum likelihood.

3.5 Sample Autocovariance Parameter Performance

To evaluate sampling protocols, we first compared their ability to detect the presence of spatial autocorrelation, given that each sample was drawn from spatially autocorrelated census data. Next, we computed $\hat{R}(h)$ for each sample for lag distances of 25, 100, and 200 m, and compared the bias and variance of these estimates relative to $R(h)$ values obtained from the census data of each basin.

We dichotomized each sample into one of two categories based on the SAC and SLR AIC values. We considered the SAC and SLR fits as competing models if the difference between their AIC values was within 2 units (Burnham and Anderson, 2002). All samples with competing models or lower SRS AIC values were classified as lacking strong evidence of spatial autocorrelation. All other samples were classified as having evidence of spatial autocorrelation. We used this dichotomization to create a response variable for each sample. Samples lacking evidence of spatial autocorrelation were assigned a value of 0, and all others were assigned a value of 1. We fit a binomial generalized linear model (GLM) to this response variable, with logit link function, to estimate the probability that each sampling protocol would yield samples with evidence of spatial autocorrelation.

Explanatory covariates in the GLM included indicator variables for sampling protocol type, and continuous basin-specific covariates to account for variation due to basins. We chose covariates that may be obtained from standard geographic information system (GIS) software. These covariates were the relative maximum distance of each sample, basin shape, the basin's drainage density, and the proportion of the basin's stream length comprised of first-order streams. Relative maximum distance is calculated by taking the maximum distance of any two locations within a sample, and dividing by the maximum distance between sampling locations from the census data for that basin. Basin shape is calculated in two steps. First, the longest straight-line distance between a basin boundary and the basin outlet is determined. Next, this value is squared and divided by the basin area (Figure 2). We also included the total number of habitat units from the census of each headwater basin. All non-sampling protocol covariates were centered at their means to allow the interpretation of the sampling protocol coefficients relative to the model intercept (GRTS sampling protocol) at the average level of all basin covariates and to minimize multicollinearity. Interactions among basin covariates and between basin covariates and sampling protocols were investigated using likelihood ratio drop in deviance tests.

Relative bias, mean-squared error (MSE), and variance for each protocol were compared for $\hat{R}(h)$ values at distances (h) of 25, 100, and 200 m. For the $j = 1 \ldots D$ samples from the ith basin for each protocol and sample size we compute relative bias as

$$Relative\ Bias = \frac{\sum_{j=1}^{D} \left(\hat{R}(h)_{j,i} - R(h)_i\right)}{R(h)_i D} \tag{6}$$

and MSE as

$$MSE = \frac{\sum_{j=1}^{D} \left(\hat{R}(h)_{j,i} - R(h)_i\right)^2}{D} \tag{7}$$

MSE is the sum of variance and the squared bias, so we also computed the variance as

$$Variance = MSE - \left(\frac{\sum_{j=1}^{D} \left(\hat{R}(h)_{j,i} - R(h)_i \right)}{D} \right)^2 \quad (8)$$

To summarize the performance of the sampling protocols, we will present the relative bias and variance values in the results section. We will also compute the relative bias for the nugget parameter for sample sizes of 48.

3.6 Distribution of Interpoint Lag Distances

A benefit of including distributed sets of clusters is to ensure both small and large lag distances among the sampling locations. Therefore, we first divided all interpoint sample distances by the largest distance within each basin. Next, we partitioned these distances into 20 bins. Finally, we computed the average proportion, across all samples and basins for each of the sampling protocols, of all inter-point distances that fell within each bin for sample sizes of 48 and 144.

4 Results

4.1 Census Data

All twelve headwater basins exhibited evidence of spatial autocorrelation via inspection of AIC values and empirical semivariograms. The magnitude of spatial autocorrelation varied among headwater basins, with autocovariance function range parameter values ranging from 351 m to 2496 m. The headwater basin census data also indicated strong nugget contributions with RSV values ranging from 0.20 to 0.55. Ten of the twelve headwater basins considered for the 48 and 72 sample sizes were best fit via traditional Euclidean distance autocovariance models, and two were best fit via in-stream distance moving average autocovariance models. Only six of the twelve basins had fish-bearing stream segments within a network of sufficient tributary junctions for consideration at sample sizes of 144. All six of the basins used for the 144 sample size analysis were best fit via Euclidean distance autocovariance models.

4.2 Sampling Protocol Performance

We present the results obtained from samples with relative maximum distances greater than 0.5, and TOCCSIC protocols from the largest cluster sizes for sample sizes of 48 and 72 ($m = 2$ and $m = 2$ and 3, respectively). The TOCCSIC protocol performance for the smallest-sized clusters at sample sizes of 48 and 72 were removed from the analysis due to very small numbers of possible samples (D).

4.2.1 Probability of Obtaining Samples with Evidence of Spatial Autocorrelation

As sample size increases, regardless of basin shape or drainage density, the estimated probability of obtaining samples with evidence of spatial autocorrelation increases (Figure 3). For sample sizes of 48, the estimated probability that a sample has evidence of spatial autocorrelation differs among sampling protocols, and there is evidence that sampling protocol behavior depends on basin covariates (Table 2). Compared to the GRTS sampling protocol, all other protocols have higher estimated probabilities of obtaining a sample with evidence of spatial autocorrelation (Figure 3), and the two cluster protocols have higher estimated probabilities than the non-cluster protocols. For all sampling protocols, the estimated probability of obtaining a sample with evidence of spatial autocorrelation is negatively associated with the number of census habitat units, headwater basin area, and the percentage of stream length comprised of first-order streams, and positively associated with the relative maximum distance of each sample (Table 2). The effect of drainage density depends on basin shape (Figure 3). Increasing drainage densities are estimated to decrease the probability of obtaining a sample with evidence of spatial autocorrelation more sharply in spherical shaped basins than linear shaped basins. At lower drainage densities, the estimated probability of obtaining a sample with spatial autocorrelation is higher in spherical basins than linear basins. The TOCCSIC sampling protocol shows lower estimated probabilities of obtaining samples with spatial autocorrelation than the Mod.GRTS protocols at higher drainage densities, regardless of basin shape (Figure 3).

For sample sizes of 72, differences among sampling protocols and associations with basin covariates (Table 3) are very similar to those observed for samples sizes of 48, although estimated probabilities of obtaining samples with evidence of spatial autocorrelation are generally higher across all sampling protocols (Figure 3). The estimated probabilities for the larger TOCCSIC ($m = 2$) samples are very similar to those from the Mod.GRTS protocols, but the probability of obtaining samples with spatial autocorrelation for smaller TOCCSIC ($m = 3$) samples is estimated to decrease more sharply with increasing drainage densities than the Mod.GRTS protocols.

At sample sizes of 144, the interacting effect of drainage density by headwater basin shape was more pronounced than that from sample sizes of 48 and 72 (Figure 3), but all sampling protocols responded similarly to changes in drainage density by basin shape (Table 4). In more linearly shaped basins, there is no estimated effect of drainage density on the probability of obtaining samples with evidence of spatial autocorrelation (Figure 3). Increasing samples sizes to 144 lead to higher estimated probabilities of obtaining samples with evidence of spatial autocorrelation across all sampling protocols compared to smaller sample sizes. The pattern among sampling protocols is similar to that observed with the smaller samples sizes, but over the majority of the drainage density range in both basin shapes the smaller TOCCSIC (m=6) cluster samples have the lowest probability of obtaining samples with evidence of spatial autocorrelation.

For all three sample sizes the Mod.GRTS protocols were among the highest probabilities of obtaining samples with evidence of spatial autocorrelation, and were less affected by increasing drainage densities in more linearly shaped basins. Except for the largest sample size, the GRTS and SRS protocols had the lowest probabilities of obtaining samples with evidence of spatial autocorrelation.

4.2.2 Bias and Variance of $\hat{R}(h)$

Overall, the bias of the GRTS and SRS protocols approached that of the cluster methods as samples sizes increased. Changes in relative bias with increasing sample size were not observed for the cluster-based sampling protocols. The variance of all protocols generally decreased as lags increased, but at 200 m few changes were observed. Across all lags and sampling protocols variance did generally decrease with increasing sample size.

Sample Size = 48

At 25 m, the GRTS sampling protocol was unbiased, the SRS protocol was slightly negatively biased, and all cluster-based sampling methods were negatively biased (Figure 4). The GRTS and SRS protocols had higher variance than the cluster-based sampling methods. At 100 m, the bias was similar among sampling protocols, but the GRTS protocol was still less biased, and the TOCCSIC protocol exhibited more negative bias than the other sampling methods. The difference in variance among sampling protocols was less pronounced than at 25 m, although TOCCSIC exhibited lower variance. At 200 m, all protocols were negatively biased, but the TOCCISC protocol was lower than the other methods. Consistent with the other distances for sample sizes of 48, the TOCCSIC also had smaller variance.

The unbiased yet highly variant nature of the GRTS and SRS protocols prompted a closer look at the relative bias of the nugget parameter. At this sample size, both the GRTS and SRS protocols demonstrated stronger negative relative bias for the nugget parameter than the cluster-based protocols (Figure 5).

Sample Size = 72

At 25 m, all Mod.GRTS and TOCCSIC protocols were negatively biased, and the GRTS and SRS protocols were less biased (Figure 6). Although the TOCCCSIC protocols showed slightly less variance, there is generally little difference among the variances of the other protocols. The pattern was similar for a lag of 100 m, but the difference in bias between the cluster-based and non-cluster based methods was smaller than at a lag of 25 m. At 200 m, the TOCCSIC protocols showed more negative bias than the other protocols, and there was generally little difference in the variances among the protocols.

Sample Size = 144

At 25 m, the GRTS and SRS were generally less biased than the cluster-based protocols, and contrary to the smaller sample sizes, the GRTS and SRS variances at 25 m were comparable to the other protocols (Figure 7). For a lag of 100 m, the TOCCSIC protocols showed more negative bias, but the box-plot quantiles of all protocols overlap, and the variance of the GRTS and 6-cluster TOCCSIC protocols were generally lower than the SRS and Mod.GRTS protocols. At 200 m, the TOCCSIC protocols showed the most negative bias and generally smaller variances. The other protocols were comparably negatively biased, but the GRTS protocols had generally smaller variance.

4.2.3 Distribution of Interpoint Lag Distances

The continuous sampling of the two cluster-based protocols lead to higher proportions of small interpoint distances compared to the GRTS and SRS protocols, but no other substantial differences were observed in other distance bins (Figure 8).

5 Discussion

Basin-specific covariate values of the 12 basins used in this study are generally representative of those from the 40 basins dataset from which the 12 were selected. With the exception of total census size, the means of all covariate values we considered were very close to mean values of those covariates from the 40-basins dataset. Mean census size for the subset of basins we analyzed was 470 and roughly 200 units higher than the overall mean of 277. Values of the basin shape covariate included the minimum and maximum values of the

40 basins, and the area covariate included the minimum and 2nd largest values. Drainage density values for the 12 basins we used included the maximum value from the 40 basins, but 7 density values from the 40 basins were smaller. Our subset included the smallest percentage of first-order stream length, but there were 5 greater values within the 40 basins than the maximum. The subset considered here was specifically selected to have sufficient fish-bearing tributaries to investigate sampling clusters located at tributary confluences.

Our investigation into the probability that each sampling protocol yields a sample with evidence of spatial autocorrelation suggests interesting notions about the role of basin structure in sampling. A stronger decrease in the probability of obtaining samples with evidence of spatial autocorrelation was observed for spherically shaped basins than linearly shaped basins. The increased number of flow-connected habitat units per distance might account for the dampened effect of increasing drainage density in more linearly shaped basins. Given a fixed area and fixed sample size, an increase in drainage density within a spherically shaped basin implies more un-flow connected habitat units, as opposed to an increasing drainage density within a more linear shaped headwater basin.

In this analysis, the extent of the sampling domain was important. Increasing values of relative maximum distance were associated with increased probabilities of a sample capturing spatial autocorrelation. Additionally, larger basins required larger samples sizes to capture spatial autocorrelation.

The preceding paragraphs present ideas that could aid scientists planning a sampling design aimed at detecting spatial autocorrelation with their samples. Considering the shape of the headwater basin, the number of habitat units with a basin, and sample attributes are important for capturing spatial autocorrelation with samples. Our results suggest that an increased sampling effort would be necessary to capture spatial autocorrelation for data collected within more spherically shaped basins, compared to linearly shaped basins with similar drainage densities. An increased effort would also be required for larger headwater basins that contained more habitat units. Our results also indicated that using samples containing clusters and samples that covered the broadest range of habitat unit distances (relative maximum distance) were more apt to capture spatial autocorrelation.

Estimation of autocorrelation functions was less affected by differences among sampling protocols than was detection of the presence of spatial autocorrelation. In general, for all sample sizes and lag distances, autocorrelation function estimates were negatively biased. This is consistent with Irvine et al. (2007), who found maximum likelihood estimates lead to underestimated autocorrelation function values when range parameters are large.

The GRTS and SRS protocols showed the least relative bias for lags of 25 m and 100 m at sample sizes of 48 and 72, but also showed larger variance, especially at sample sizes of 48. This is likely due to the severe negative relative bias of the nugget parameter for the GRTS and SRS protocols. A similar, though less extreme, difference was observed for the nugget parameter for samples sizes of 72. As noted in Section 2, the divisor of the autocorrelation function contains the nugget parameter, and severe underestimation of the nugget will inflate autocorrelation estimates. The GRTS and SRS protocols were less likely to result in samples with evidence of spatial autocorrelation. When samples were spatially autocorrelated, nugget values were small. The lack of sample points occurring at the smallest lag distances might explain the inability for proper nugget parameter estimation at smaller sample sizes, but the cluster based protocols had more small interpoint distances at sample sizes of 144 when relative bias values were generally consistent among protocols.

Tributary junctions were indeed sources of heterogeneity, and seemingly too heterogeneous for effective estimation of spatial autocovariance parameters. The smallest TOCCSIC clusters at sample sizes of 48 and 72 were most affected by changes in drainage density and had the lowest estimated probability of yielding samples with evidence of spatial autocorrelation at sample sizes of 144. Only the larger-clustered TOCCSIC protocol performance was comparable to the Mod.GRTS generated samples, when the three "arms" of the TOCCSIC clusters extended further into the three stream segments joining at each tributary junction. Smaller-clustered TOCCSIC samples were, generally, the most negatively biased among the sampling protocols.

The cluster sizes we considered could be a reason we did not see superior performance from our cluster-based sampling protocols in regards to estimation of autocorrelation function parameters. At the onset, we were interested in comparing Mod.GRTS and TOCCSIC clusters containing the same number of habitat units. We therefore restricted our cluster-based sampling designs to contain small numbers of large clusters. The designs deemed optimal by Zimmerman (2006) and Zhu and Stein (2005) contained many more, and hence, smaller, clusters distributed across the sampling domain, and those of Zhu and Zhang (2006) contained several clusters of varying sizes and non-clustered sampling locations. An investigation comparing GRTS, larger numbers of smaller-sized Mod.GRTS, and a combination of GRTS and Mod.GRTS might prove useful. This would more closely mimic the cluster sizes and distributions of these studies. It would also allow more of the 40 headwater basins to be used by eschewing the need to consider the number of tributary confluences.

Variation among basins could be another reason for not observing more distinct bias and variance differences among sampling protocols. In particular, sample sizes represented different proportions of the census size from each basin. The average number of census habitat units was 470 for the 12 basins used for sample sizes of 48 and 72 (range: 195 - 713). Analyses for sample sizes of 144 were conducted with 6 basins, whose number of habitat units ranged from 340 to 713 (five of six had more than 600 habitat units). As sample size became a smaller proportion of the census size, the probability of obtaining a sample with autocorrelation decreased. To generalize the relative merits of sampling designs for autocovariance parameter estimation across streams, we considered a broad set of census sizes, but this may have clouded our ability to detect differences.

Our investigation is based on the assumption that the goal of the analysis is to estimate the spatial autocovariance function to describe the spatial pattern within headwater basins. If the analysis goal is estimating autocovariance parameters for prediction of fish counts in habitat units, both Zhu and Stein (2005) and Zimmerman (2006) suggest that regularly spaced sample points, that also contain several small clusters, may be optimal. This differs from their recommendations for the estimation of autocovariance function parameters in which all sample points are within clusters. The GRTS and Mod.GRTS combination described above may also prove fruitful for an investigation regarding sampling designs for optimal prediction performance.

Only two of the basins considered here were best fit by up-stream moving average models. Further developments have led to valid moving average autocovariance models that incorporate both flow-connected and unconnected locations (Garreta et al., 2009). These may be more appropriate for lotic organisms, like fish, that are capable of moving up and downstream. If only up-stream moving average models are considered, utilizing some larger TOCCSIC samples within a broader sampling plan may help improve autocovariance parameter estimation. TOCCSIC samples do ensure a sample would contain flow-connected locations, and also provide better nugget parameter estimation via clustering.

Our analyses demonstrate that implementing a GRTS sampling protocol may be sensible if obtaining spatially distributed samples without spatial autocorrelation is of interest, especially when the sample size is small compared to census size. The GRTS protocol did have lower estimated probabilities of obtaining samples with evidence of spatial autocorrelation than even the SRS protocol. Additionally, the GRTS protocol would provide a spatially distributed sample.

In terms of estimating autocovariance function parameters in headwater stream networks, implementing a sampling protocol that includes a spatially distributed set of large clusters, akin to the Mod.GRTS framework we proposed, may be preferred because better nugget estimation performance can be expected. There remains substantial room for refinement in regards to general results for optimal sampling designs across heterogeneous systems such as headwater stream networks.

6 Acknowledgements

Research supported in part by the Fish and Wildlife in Managed Forests Research Program: Oregon State University Forest Research Laboratory, and the

Watersheds Research Cooperative. Any use of trade, product, or firm names is for descriptive purposes only and does not imply endorsement by the U.S. Government. The authors thank Jay Ver Hoef for useful discussion regarding the analysis. Two anonymous reviewers provided comments that improved the manuscript.

References

Bateman DS, Gresswell RE, Torgersen CE. 2005. Evaluating single-pass catch as a tool for identifying spatial pattern in fish distribution. *Journal of Freshwater Ecology* **20**: 335–345.

Benda L, Andras K, Miller D, Bigelow P. 2004a. Confluence effects in rivers: Interactions of basin scale, network geometry, and disturbance regimes. *Water Resources Research* **40**:

Benda L, Poff NL, Miller D, Dunne T, Reeves G, Pess G, Pollock M. 2004b. The Network Dynamics Hypothesis: How Channel Networks Structure Riverine Habitats. *BioScience* **54**(4): 413–427.

Blair BC. 2005. Fire effects on the spatial patterns of soil resources in a Nicaraguan wet tropical forest. *Journal of Tropical Ecology* **21**: 435–444.

Bouza N, Caujape-Castells J, Gonzalez-Perez MA, Batista F, Sosa PA. 2002. Population structure and genetic diversity of two endangered endemic species of the Canarian laurel forest: *Dorycnim spectabile (fabaceae)* and *Isoplexis chalcantha (scrophulariaceae)*. *International Journal of Plant Sciences* **163**(4): 619–630.

Bulit C, Diaz-Avalos C, Montagnes DJS. 2004. Assessing spatial and temporal patchiness of the autotrophic ciliate *Myrionecta rubra*: a case study in a coastal lagoon. *Marine Ecology Progress Series* **268**: 55–67.

Bulit C, Diaz-Avalos C, Signoret M, Montagnes DJS. 2003. Spatial structure of planktonic ciliate patches in a tropical coastal lagoon: an application of geostatistical methods. *Aquatic Microbial Ecology* **30**: 185–196.

Burnham KP Anderson DR. 2002. *Model Selection and Multimodel Inference: A Practical InformationTheoretic Approach*, New York, NY: Springer-Verlag, 2nd ed.

Cooper SD, Barmuta L, Sarnelle O, Kratz K, Diehl S. 1997. Quantifying Spatial Heterogeneity in Streams. *Journal of the North American Benthological Society* **16**(1): 174–188.

Cressie N, Frey J, Harch B, Smith M. 2006. Spatial Prediction on a River Network. *Journal of Agricultural, Biological, and Environmental Statistics* **11**(2): 127–150.

Cressie N Majure JJ. 1997. Spatio-Temporal Statistical Modeling of Livestock Waste in Streams. *Journal of Agricultural, Biological, and Environmental Statistics* **2**(1): 24–47.

Dent CL Grimm NB. 1999. Spatial heterogeneity of stream water nutrient concentrations over successional time. *Ecology* **80**(7): 2283–2298.

Downes BJ, Lake PS, Schreiber ESG. 1993. Spatial variation in the distribution of stream invertebrates: implications of patchiness for models of community organization. *Freshwater Biology* **30**: 119–132.

Ettema CH Wardle DA. 2002. Spatial soil ecology. *TRENDS in Ecology & Evolution* **17**(4): 177–183.

Ferguson RI, Cudden JT, Hoey TB, Rice SP. 2006. River system discontinuities due to lateral inputs: generic styles and controls. *Earth Surface Processes and Landforms* **31**: 1149–1116.

Ganio LM, Torgersen CE, Gresswell RE. 2005. A Geostatistical Approach for Describing Spatial Pattern in Stream Networks. *Frontiers in Ecology and the Environment* **3**(3): 138–144.

Gardner B, Sullivan PJ, Arthur Jr. JL. 2003. Predicting Stream Temperatures: Geostatistical Model Comparison Using Alternative Distance Metrics. *Canadian Journal of Fisheries and Aquatic Sciences* **60**: 344–351.

Garreta V, Monestiez P, Ver Hoef JM. 2009. Spatial modelling and prediction on river networks: up model, down model or hybrid? *Environmetrics* .

Gascuel-Odoux C Boivin P. 1994. Variability of variograms and spatial estimates due to soil sampling: a case study. *Geoderma* **62**: 165–182.

Gresswell RE, Bateman DS, Lienkaemper GW, Guy TJ 2004. Geospatial Techniques for Developing a Sampling Frame of Watersheds Across a Region. in *GIS/Spatial Analyses in Fishery and Aquatic Sciences*, eds. Nishida T, Kailola PJ, Hollingworth CE, Fishery-Aquatic GIS Research Group, Saitama, Japan, vol. 2, pp. 515–528.

Gresswell RE, Torgersen CE, Bateman DS, Guy TJ, Hendricks SR, Wofford JEB 2006. A spatially explicit approach for evaluating relationships among coastal cutthroat trout, habitat, and disturbance in headwater streams. in *Influences of landscapes on stream habitats and biological assemblages*, eds. Hughes R, Wang L, Seelbach P, Bethesda, Maryland: American Fisheries Society, pp. 457–471.

Grundmann GL Debouzie D. 2000. Geostatistical analysis of the distribution of NH4+ and NO3- -oxidizing bacteria and serotypes at the millimeter scale along a soil transect. *FEMS Microbiology Ecology* **34**: 57–62.

Huettmann F Diamond AW. 2006. Large-scale effects on the spatial distribution of seabirds in the Northwest Atlantic. *Landscape Ecology* **21**: 1089–1108.

Hynes HBN. 1975. The Stream and its Valley. *Internationale Vereinigung fr Theoretische und Angewandte Limnologie* **19**: 1–15.

Irvine KM, Gitelman AI, Hoeting JA. 2007. Spatial Designs and Properties of Spatial Correlation: Effects on Covariance Estimation. *Journal of Agricultural, Biological, and Environmental Statistics* **12**(4): 450–469.

Isaak DJ Thurow RF. 2006. Network-Scale Spatial and Temporal Variation in Chinook Salmon (*Oncorhynchus tshawutscha*) Redd Distributions: Patterns Inferred from Spatially Continuous Replicate Surveys. *Canadian Journal of Fisheries and Aquatic Sciences* **63**: 285–296.

Kiffney PM, Greene CM, Hall JE, Davies JR. 2006. Tributary streams create spatial discontinuities in habitat, biological productivity, and diversity in mainstem rivers. *Canadian Journal of Fisheries and Aquatic Sciences* **63**: 2518–2530.

Kincaid T, Olsen TwcfDS, Platt C, White D, Remington R 2008. *spsurvey: Spatial Survey Design and Analysis*, r package version 2.0.

Legendre P. 1993. Spatial Autocorrelation: Trouble or New Paradigm? *Ecology* **74**(6): 1659–1673.

Little LS, Edwards D, Porter DE. 1997. Kriging in Estuaries: as the Crow Flies, or as the Fish Swims? *Journal of Experimental Marine Biology and Ecology* **213**: 1–11.

Lloyd NJ, Mac Nally R, Lake PS. 2005. Spatial Autocorrelation of Assemblages of Benthic Invertebrates and its Relationship to Environmental Factors in Two Upland River in Southeastern Australia. *Diversity and Distributions* **11**: 375–386.

Mast JN Veblen TT. 1999. Tree spatial patterns and stand development along the pinegrassland ecotone in the Colorado Front Range. *Canadian Journal of Forest Research* **29**: 575–584.

Muller WG Zimmerman DL. 1999. Optimal designs for variogram estimation. *Environmetrics* **10**: 23–37.

Muneto H, Ohte N, Karasawa N, Zhang Gs, Wang Lh, Yoshikawa K. 2001. Plant Species Effect on the Spatial Patterns of Soil Properties in the Mu-us Desert Ecosystem, Inner Mongolia, China. *Plant and Soil* **234**: 195–205.

Neville HM, Isaak DJ, Dunham JB, Thurow RF, Rieman BE. 2006. Fine-scale natal homing and localized movement as shaped by sex and spawning babitat in Chinook salmon: insights from spatial autocorrelation analysis of individual genotypes. *Molecular Ecology* **15**: 4589–4602.

Peterson EE, Theobald DM, Ver Hoef JM. 2007. Geostatistical Modelling on Stream Networks: Developing Valid Covariance Matrices Based on Hydrologic Distance and Stream Flow. *Freshwater Biology* **52**: 267–279.

Peterson EE Urquhart NS. 2006. Predicting Water Quality Impaired Stream Segments Using Landscape-Scale Data and a Regional Geostatistical Model: A Case Study in Maryland. *Environmental Monitoring and Assessment* **121**: 615–638.

Pickett STA Cadenasso ML. 1995. Landscape Ecology: Spatial Heterogeneity in Ecological Systems. *Science* **269**: 331–334.

Poole GC. 2002. Fluvial Landscape Ecology: Addressing Uniqueness within the River Discontinuum. *Freshwater Biology* **47**: 641–660.

Pooler PS Smith DR. 2005. Optimal sampling design for estimating spatial distribution and abundance of a freshwater mussel population. *Journal of the North American Benthological Society* **24**(3): 525–537.

R Development Core Team 2005. *R: A language and environment for statistical computing*, R Foundation for Statistical Computing, Vienna, Austria, ISBN 3-900051-07-0.

Rathbun SL. 1998. Spatial Modelling in Irregularly Shaped Regions: Kriging Estuaries. *Environmetrics* **9**: 109–129.

Rice S Church M. 1998. Grain size along two gravel-bed rivers: statistical variation, spatial pattern and sedimentary links. *Earth surface processes and landforms* **23**: 345–363.

Rice SP, Ferguson RI, Hoey TB. 2006. Tributary control of physical heterogeneity and biological diversity at river confluences. *Canadian Journal of Fisheries and Aquatic Sciences* **63**: 2553–2566.

Rossi JP. 2003. Clusters in Earthworm Spatial Distribution. *Pedobiologia* **47**: 490–496.

Russo D Bresler E. 1981. Soil hydraulic properties as stochastic processes: I. An analysis of field spatial varability. *Soil Science Society of America Journal* **45**: 682–687.

Russo D Jury WA. 1987. A Theoretical Study of the Estimation of the Correlation Scale in Spatially Variable Fields 1: Stationary Fields. *Water Resources Research* **23**(7): 1257–1268.

Schabenberger O Gotway CA. 2005. *Statistical Methods for Spatial Data Analysis*, Texts in Statistical Science Series, Boca Raton, FL: Chapman and Hall/CRC.

Schlesinger WH, Raikes JA, Hartley AE, Cross AF. 1996. On the Spatial Pattern of Soil Nutrients in Desert Ecosystems. *Ecology* **77**(2): 364–374.

Solie JB, Raun WR, Stone ML. 1999. Submeter Spatial Variability of Selected Soil and Bermudagrass Production Variables. *Soil Science Society of America Journal* **63**: 1724–1733.

Stevens Jr. D Olsen AR. 2004. Spatially balanced sampling of natural resources. *Journal of the American Statistical Association* **99**(465): 262–278.

Torgersen CE Close DA. 2004. Influence of Habitat Heterogeneity on the Distribution of Larval Pacific Lamprey (*Lampetra tridentata*) at Two Spatial Scales. *Freshwater Biology* **49**(5): 614–630.

Torgersen CE, Gresswell RE, Bateman DS, Burnett KM 2008. Spatial identification of tributary impacts in river networks. in *River confluences, tributaries and the fluvial network*, eds. Rice SP, Roy AG, Rhoads BL, London: Wiley, pp. 159–182.

Venditti JG Church MA. 2005. Bed form initiation from a flat sand bed. *Journal of Geophysical Research* **110**:

Ver Hoef JM, Peterson E, Theobald D. 2006. Spatial Statistical Models that use Flow and Stream Distance. *Environmental and Ecological Statistics* **13**: 449–464.

Ver Hoef JM Peterson EE 2007. Spatial Modeling of Stream Network Data. in *Proceedings of the 92nd Annual Meeting of the Ecological Society of America*, San Jose, CA.

Zhu Z Stein ML. 2005. Spatial sampling design for parameter estimation of the covariance function. *Journal of Statisitcal Planning and Inference* **134**: 583–603.

Zhu Z Zhang H. 2006. Spatial sampling design under the infill asymptotic framework. *Environmetrics* **17**(4): 323–337.

Zimmerman DL. 2006. Optimal network design for spatial prediction, covariance parameter estimation, and empirical prediction. *Environmetrics* **17**: 635–652.

Zuur AF, Ieno EN, Walker NJ, Saveliev AA, Smith GM. 2009. *Mixed Effects Models and Extensions in Ecology with R*, Statistics for Biology and Health, New York, NY: Springer, 3rd ed.

Table 1: Sample sizes by number of clusters and cluster size.

Sample Size n	Number of Clusters m	Cluster Size l
48	2	24
	4	12
72	2	36
	3	24
	4	18
	6	12
144	4	36
	6	24

Table 2: Estimated effects of basin covariates and sampling protocols on the odds a sample has spatial autocorrelation for sample sizes equal to 48.

Variable	Estimate	Std. Error	Effect*	Lower 95% CI*	Upper 95% CI*
Intercept	-1.9257	0.1251	0.1458	0.1141	0.1863
Census Size	-0.0018	0.0003	0.9142	0.8887	0.9403
Drainage Density	-3.0485	0.3375	0.0474	0.0245	0.0919
Basin Shape	0.1473	0.0636	1.1587	1.0230	1.3124
Area (km^2)	-0.3912	0.0548	0.9068	0.8828	0.9315
First-order Percentage	-7.7055	0.9419	0.0005	0.0001	0.0029
Sample Rel. Max. Dist	3.1750	0.5635	1.0323	1.0209	1.0437
Mod. GRTS-2	1.7468	0.2189	5.7362	3.7350	8.8097
Mod. GRTS-4	2.1011	0.2028	8.1753	5.4940	12.1653
SRS	0.5338	0.1346	1.7054	1.3100	2.2201
TOCCSIC-2	1.6933	0.4323	5.4373	2.3303	12.6869
DrainDens*Basin Shape	1.7294	0.2098	5.6375	3.7365	8.5057
DrainDens*Mod.GRTS-2	0.9904	0.4129	2.6922	1.1984	6.0479
DrainDens*Mod.GRTS-4	0.4815	0.3566	1.6185	0.8046	3.2559
DrainDens*SRS	0.0236	0.3373	1.0238	0.5286	1.9831
DrainDens*TOCCSIC-2	-0.6286	0.8776	0.5333	0.0955	2.9787

*Odds effects represent 50-unit increases in basin census size, 0.25-km^2 increases in basin area, and 10-m increases in relative maximum distance.

Table 3: Estimated effects of basin covariates and sampling protocols on the odds a sample has spatial autocorrelation for sample sizes equal to 72.

Variable	Estimate	Std. Error	Effect*	Lower 95% CI*	Upper 95% CI*
Intercept	-1.1660	0.1171	0.3116	0.2477	0.3920
Census Size	-0.0025	0.0003	0.8825	0.8597	0.9059
Drainage Density	-3.6388	0.2814	0.0263	0.0151	0.0456
Basin Shape	0.4976	0.0628	1.6449	1.4545	1.8601
Area (km^2)	-0.4145	0.0484	0.9016	0.8804	0.9232
First-order Percentage	-9.2341	0.8137	0.0001	0.0000	0.0005
Sample Rel. Max. Dist	4.8425	0.4507	1.0496	1.0404	1.0589
Mod. GRTS-2	1.8886	0.1973	6.6101	4.4900	9.7311
Mod. GRTS-3	1.8408	0.1770	6.3014	4.4541	8.9150
Mod. GRTS-4	2.0083	0.1791	7.4506	5.2449	10.5839
Mod. GRTS-6	2.0342	0.2062	7.6460	5.1045	11.4528
SRS	0.5223	0.1242	1.6858	1.3216	2.1505
TOCCSIC-2	2.1648	0.3660	8.7128	4.2524	17.8520
TOCCSIC-3	1.5957	0.2548	4.9317	2.9930	8.1260
DrainDens*Basin Shape	1.0995	0.1908	3.0026	2.0656	4.3646
DrainDens*Mod.GRTS-2	1.5453	0.3721	4.6894	2.2616	9.7235
DrainDens*Mod.GRTS-3	1.7947	0.3095	6.0178	3.2807	11.0388
DrainDens*Mod.GRTS-4	1.0335	0.2939	2.8110	1.5801	5.0008
DrainDens*Mod.GRTS-6	0.6612	0.3804	1.9372	0.9191	4.0831
DrainDens*SRS	0.0968	0.3055	1.1017	0.6054	2.0048
DrainDens*TOCCSIC-2	0.6907	0.6432	1.9952	0.5656	7.0385
DrainDens*TOCCSIC-3	-0.8164	0.4784	0.4420	0.1731	1.1290

*Odds effects represent 50-unit increases in basin census size, 0.25-km^2 increases in basin area, and 10-m increases in relative maximum distance.

Table 4: Estimated effects of basin covariates and sampling protocols on the odds a sample has spatial autocorrelation for sample sizes equal to 144.

Variable	Estimate	Std. Error	Effect*	Lower 95% CI*	Upper 95% CI*
Intercept	0.4853	0.1766	1.6247	1.1494	2.2964
Drainage Density	-1.8114	0.1402	0.1634	0.1242	0.2151
Basin Shape	-1.2609	0.2793	0.2834	0.1639	0.4899
Sample Rel. Max. Dist	7.4422	0.7476	1.0773	1.0616	1.0932
Mod. GRTS-4	1.7568	0.2926	5.7937	3.2649	10.2811
Mod. GRTS-6	1.5483	0.3107	4.7034	2.5584	8.6468
SRS	0.2420	0.2101	1.2738	0.8439	1.9226
TOCCSIC-4	2.0339	0.3213	7.6438	4.0723	14.3476
TOCCSIC-6	-0.0141	0.2688	0.9860	0.5822	1.6699
DrainDens*Basin Shape	3.7200	0.5166	41.2640	14.9919	113.5754

*Odds effects represent 10-m increases in relative maximum distance.

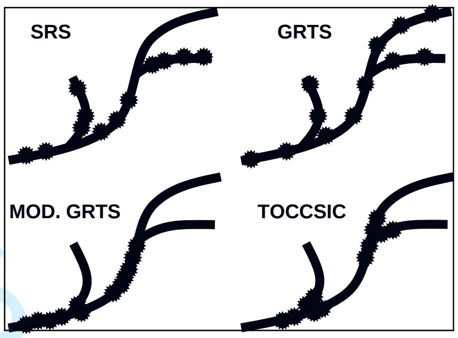

Figure 1: Basic representations of each sampling protocol.

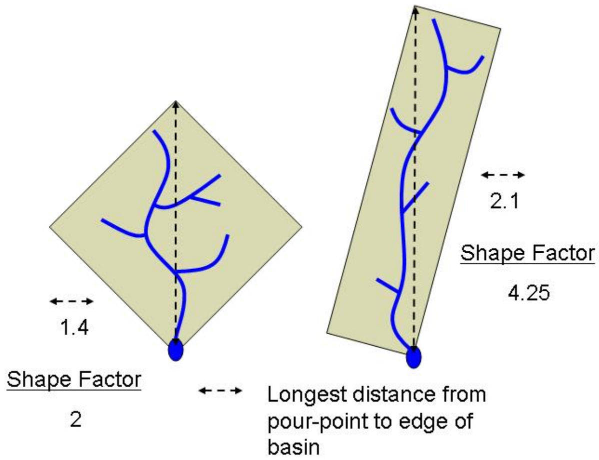

Figure 2: Examples of shape factor calculation. Each basin has area equal to 1 unit^2.

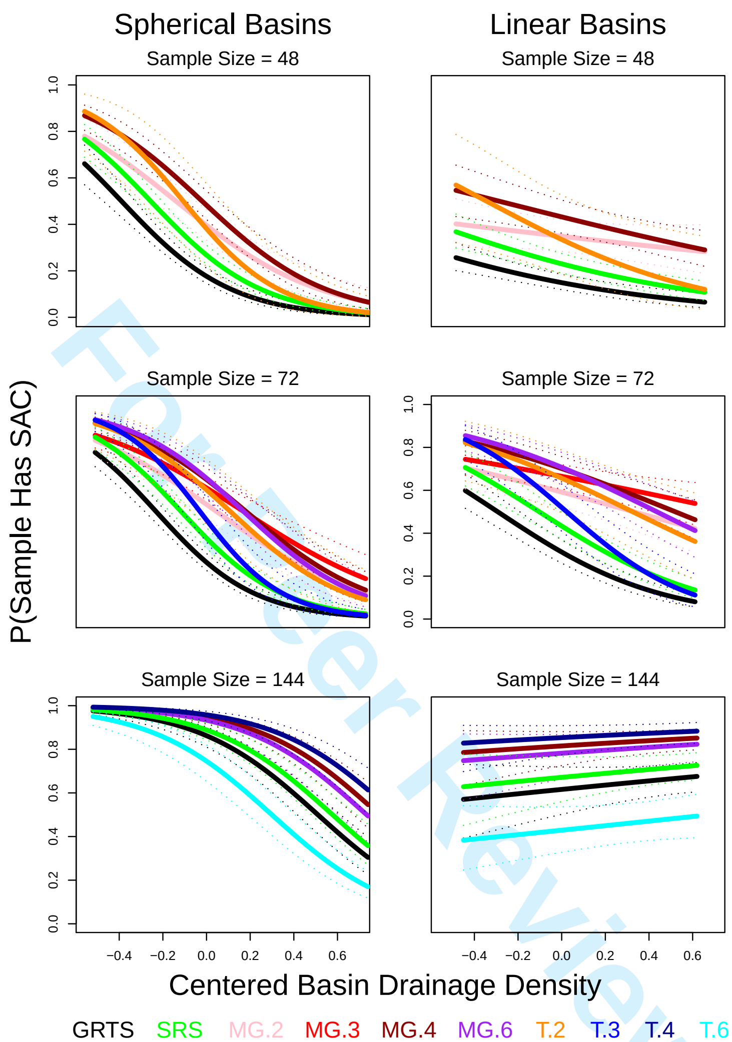

Figure 3: Effects of sampling design and headwater basin drainage density on the probability that samples contain spatial autocorrelation, by basin shape. In each graph the relative maximum distance is set to the average of each sampling protocol. The first-order percentage, maximum census size, and headwater basin areas are set to the average within each basin shape. The x-axis in each plot represents the range of centered drainage densities within each shape, and the spherical-shaped basins span a slightly larger range of values. Dotted lines represent 95% confidence intervals.

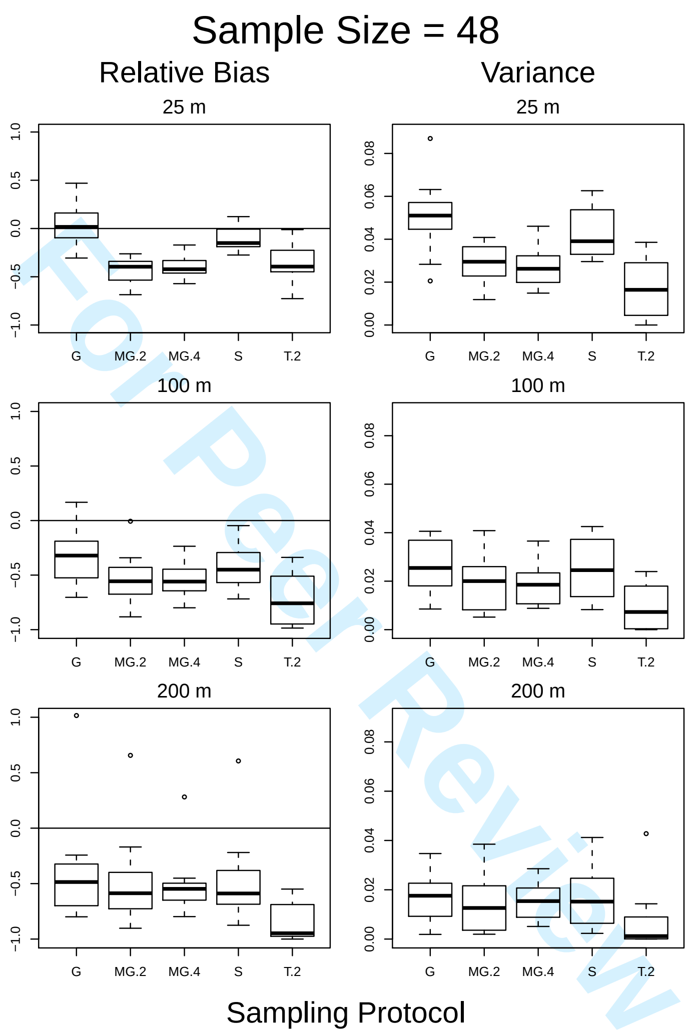

Figure 4: Relative bias and variance of estimating the autocorrelation function at 25 m, 100 m, and 200 m for sample sizes of 48 and GRTS (G), SRS (S), Mod. GRTS (MG.x) and TOCCSIC (T.x) sampling protocols. .x refers to the number of clusters. Each protocol includes values calculated at each basin.

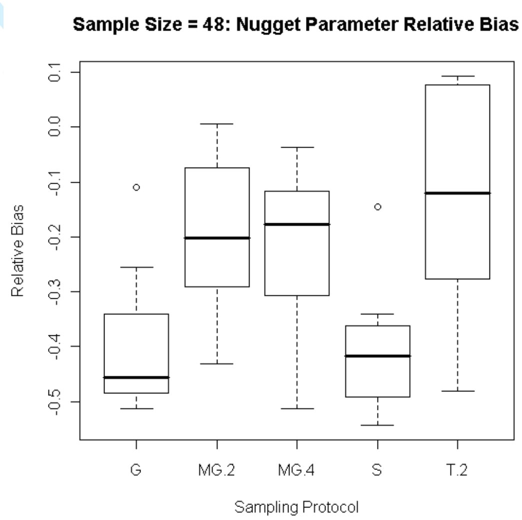

Figure 5: Relative bias of the nugget parameter for sample sizes of 48 and GRTS (G), SRS (S), Mod. GRTS (MG.x) and TOCCSIC (T.x) sampling protocols. .x refers to the number of clusters. Each protocol includes values calculated at each basin.

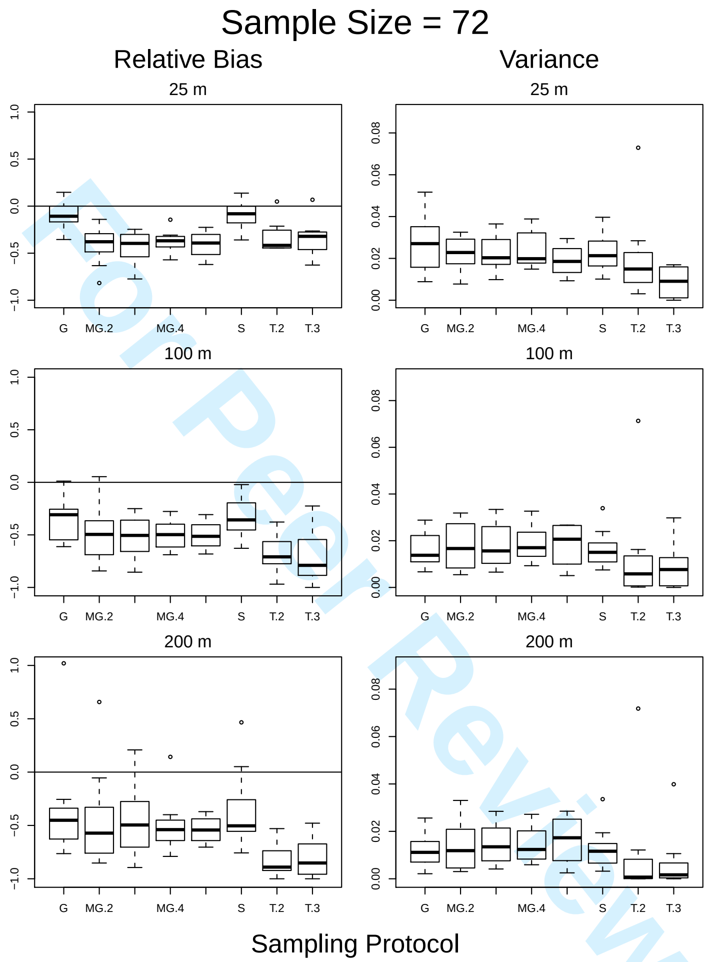

Figure 6: Relative bias and variance of estimating the autocorrelation function at 25 m, 100 m, and 200 m for sample sizes of 72 and GRTS (G), SRS (S), Mod. GRTS (MG.x) and TOCCSIC (T.x) sampling protocols. .x refers to the number of clusters. Each protocol includes values calculated at each basin.

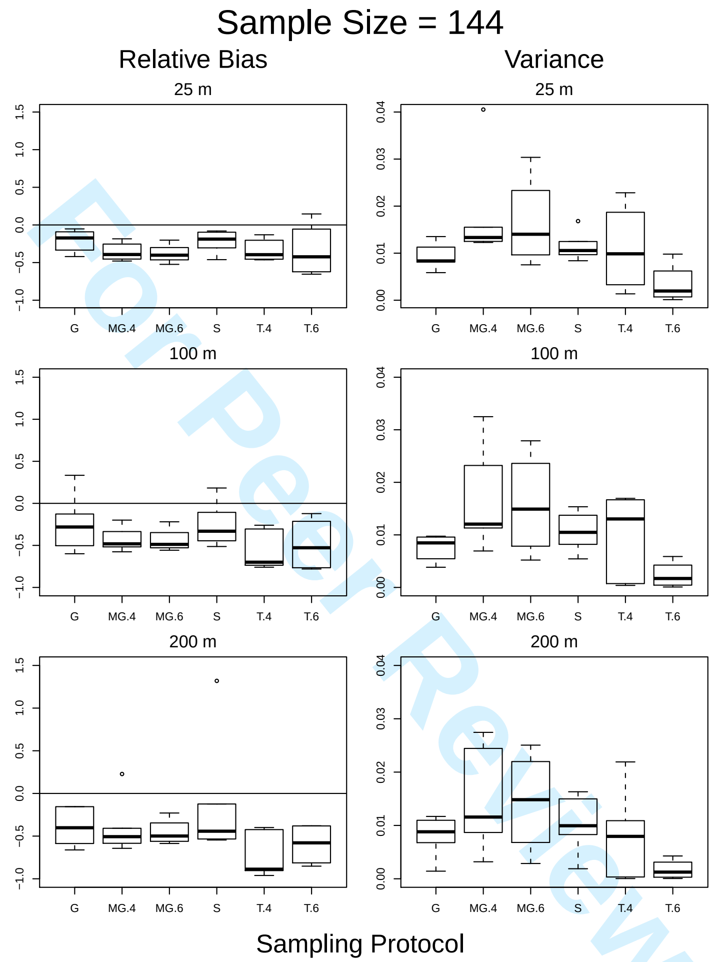

Figure 7: Relative bias and variance of estimating the autocorrelation function at 25 m, 100 m, and 200 m for sample sizes of 144 and GRTS (G), SRS (S), Mod. GRTS (MG.x) and TOCCSIC (T.x) sampling protocols. .x refers to the number of clusters. Each protocol includes values calculated at each basin.

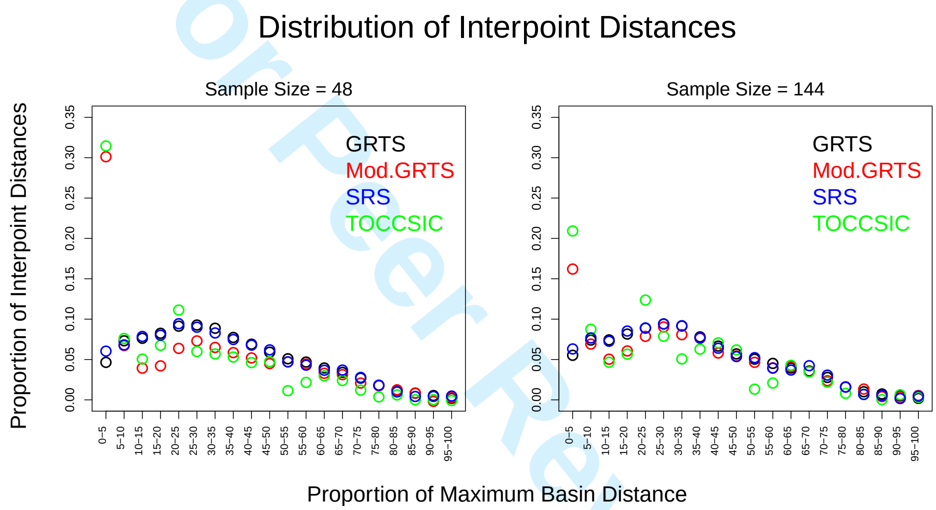

Figure 8: Distribution of interpoint relative distances averaged by sampling protocol and across all headwater basins, for sample sizes of 48 and 144.